

## *In situ* Raman Analysis of Lithium-Ion Batteries

### Abstract

The needs of the Li-ion battery customers can be segmented into *in situ* and *ex situ* modes of analysis. *In situ* analysis allows researchers to follow changes in a battery cell during its charge and discharge cycles. Recent improvements in Raman sensitivity enable these changes to be imaged on a dynamic time scale.

### Introduction

The use of Raman spectroscopy to analyze battery materials has been around for years. During the 1960s, researchers used Raman spectroscopy to elucidate many of the fundamental spectral features of the minerals and inorganic materials widely used in battery research today.<sup>1,2</sup> Raman spectroscopy is a good fit for these materials because many of the characteristic vibrational and rotational modes occur in the low-wavenumber region of the spectrum, typically accessible only by far-infrared measurements. In the past, both Raman and far-infrared (FIR) measurements were time-consuming and difficult experiments.

Advances in instrumentation have significantly increased the ease of use, making Raman techniques a much more approachable. New areas of application ensued, such as the exploding interest in rechargeable lithium-ion batteries. Many researchers are involved and have published careful studies of materials specifically related to Li-ion batteries and next-generation batteries. The review articles published by Julien in 2018 and Baddour-Hadjean in 2010 are excellent resources for those wishing to learn more about the developments in this field.<sup>3, 12</sup> This application note focuses on the *in situ* application of Raman spectroscopy as it pertains to battery research.



Thermo Scientific DXR3xi Raman Imaging Microscope

### Analysis techniques: *in situ* versus *ex situ*

The term *in situ* is used to describe experiments in which the battery components are studied in an assembled cell under operating conditions. Think of *in situ* as the window to the chemical reactions that happen inside a battery, such as charging and discharging a battery. There are very few commercially available cell designs compatible with spectroscopic measurements. Researchers have resorted to building their own cells to meet the needs of their experimental apparatus. Examples of such designs have been published along with experimental results.<sup>4-10, 13</sup>

*In situ* cells analysis is generally targeted at researching and developing new materials for Li-ion batteries. Once a formulation is designed, a candidate battery is scaled up through pilot production to actual product samples. At this stage of development, researchers are most interested in characterizing failure modes and a better understanding of performance differences. For example, what makes one production run work better than another, and why did one battery fail yet its siblings from the same batch work fine?

To answer these questions, researchers must carefully disassemble a battery cell to examine the individual components. This type of analysis is called *ex situ* because the battery components are removed from the operating battery cell. The goal is to prepare the samples for analysis in as close to a native state as possible. Please see the companion application note for details on *ex situ* analysis.

### From single point measurements to Raman imaging

The majority of published research on Li-ion battery *in situ* Raman work is based on single point measurements acquired over time during charge/discharge cycles. An example is the excellent work done by Kostecki's group at Lawrence Berkeley National Lab.<sup>11</sup>

Single point measurements can be misleading because there is no way of knowing if the sampled point is representative of the entire electrode. It is important to make multiple measurements to be sure. Because the Raman signals are weak, it takes many minutes to generate enough signal-to-noise ratio at each measurement point. A complete, multi-point experiment can be quite time-consuming to complete.

Today, Raman imaging is a viable alternative that enables you to quickly make thousands of measurements over an area of the electrode rather than just single point measurements. Each pixel in a Raman image is a complete Raman spectrum, so you can observe if changes are heterogeneous or hot spots.

The following experimental results demonstrate the flexibility of using Raman spectroscopy for *in situ* analysis of Li-ion batteries and their components.

### Lithiation of graphite

Graphite is widely used as an anode material for rechargeable Li-ion batteries.

During the Li-ion battery charging cycle, positively charged Li<sup>+</sup> ions move from the cathode through the electrolyte, across a separator into the anode to balance the flow of electrons in the external circuit (Figure 1). This process of Li<sup>+</sup> ions entering the graphitic structure of the anode is called intercalation. Intercalation causes changes in the anode structure – primarily a swelling of the graphite structure.

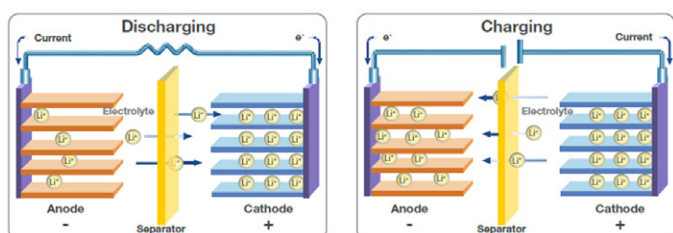


Figure 1. Movement of Li<sup>+</sup> ions balance electrons during the charge and discharge cycles of a Li-ion battery.

### Experimental

The experimental setup for this example consists of a Thermo Scientific™ DXR™xi Raman Imaging Microscope and an ELCELL® ECC-Opto-Std Optical Electrochemical Cell. This cell enables the investigation of batteries in a “sandwich” configuration where the working electrode (WE) material is placed under a sapphire (Al<sub>2</sub>O<sub>3</sub>) window. In this example, the electrode material (graphite powder) is spread onto a copper grid serving as the current collector. This WE is sandwiched from below, with a glass fiber separator soaked with the electrolyte solution and lithium metal as the counter electrode (CE).

The Raman beam from the microscope objective impinges onto the backside of the WE material through the sapphire window (Figure 2). The advantage of investigating the backside of the electrode is that the pathway for the Raman beam is minimized, allowing the use of high magnification objectives to optimize spectra quality. The drawback is the gradient of lithiation concentration along the depth of the electrode. Accordingly, the electrode must be charged very slowly to minimize this unwanted gradient.

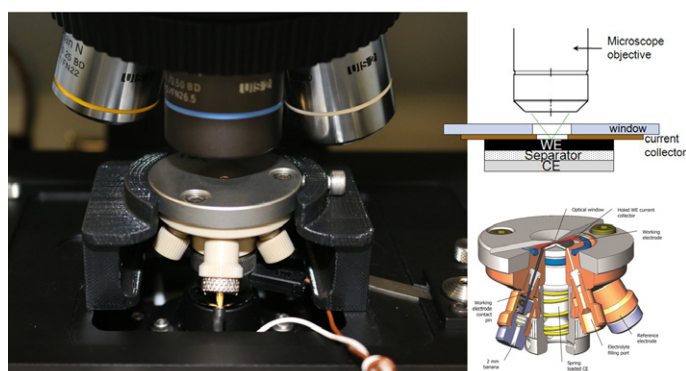


Figure 2. Experimental setup for the *in situ* example showing the electrochemical cell mounted on a Raman imaging microscope stage.

The graphite electrode was cycled at a constant rate of approximately 0.06 C. The C-rate measures how rapidly a battery is charged/discharged. This rate of 0.06 C corresponds to 33 hours for a complete charge/discharge cycle between 1.5 and 0.005 V against Li/Li<sup>+</sup>. Raman imaging was carried out during the initial 480 minutes of the charging (lithiation) process only.

Raman spectra were collected over a 30 μm × 30 μm area at 1 μm pixel spacing using two mW of 532 nm laser excitation, a 0.01 sec exposure time for each pixel, and 50 scans per image. Higher laser powers and/or longer exposure times resulted in the burning of the graphite and boiling of the electrolyte.

## Results

A Raman image is a hyperspectral dataset, with each pixel in the image being a complete Raman spectrum. This hyperspectral Raman data uses various spectral processing techniques to generate image contrast pertaining to specific chemical features. It is this capability that visualizes minute differences within a sampled area. By collecting a sequence of Raman images, we now can monitor changes in both space and time. As mentioned earlier, various chemical images can be created from each dataset showing changes within the sampled area. Alternatively, the Raman spectral data within each dataset can be averaged to produce a single spectrum for each time slice. In this mode, the Raman imaging dataset is used as a means of homogenizing any differences in the electrode area. This average spectrum represents a single point measurement, yet each point represents a 30  $\mu\text{m}$  square compared with the typical 1  $\mu\text{m}$  sample area from a standard Raman microscope.

In Figure 3, the 3D view (bottom left) shows changes in the Raman spectrum as a function of time over 8.3 hours (1–500 min). During this time, the battery cell is in the charging (lithiation) process only. This portion of the electrochemical cycle is shown in the lower right of Figure 3.

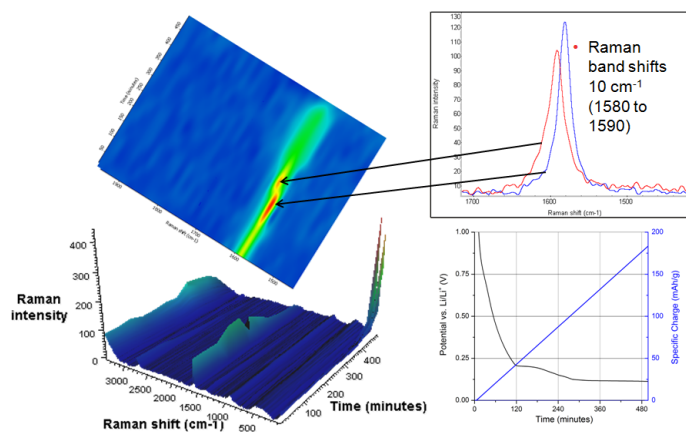


Figure 3. Different views rendered from the time lapse hyperspectral Raman data provide a wealth of experimental information.

The spectrum of graphite exhibits a prominent peak at 1580  $\text{cm}^{-1}$  attributed to the  $E_{2g2}$  mode (G-band). At potentials between 0.42 and 0.31 V (specific charge 33 and 45 mAh/g), the band gradually disappears along with the simultaneous emergence of a peak centered at 1590  $\text{cm}^{-1}$ . This peak shift is attributed to the  $\text{Li}^+$  ions intercalated into the graphite structure. This is more easily seen in the center, 2D Raman image. The inset shows Raman spectra before and after the change.

Toward the end of the charge cycle at 8.3 hours (496 min), where the voltage is less than 0.15 V (specific charge greater than 146 mAh/g), a strong Raman band centered at 154  $\text{cm}^{-1}$  begins to appear. This Raman band has not been previously reported, so its assignment is not conclusive. Strong Raman bands in this region have been attributed to  $\text{TiO}_2$ , Sb, and metal chlorides.

The type of views shown in Figure 3 are “spectrum-centric” because they show changes in the Raman spectra captured at different times during a time-based analysis. Figure 4 shows another way of exploring the same Raman imaging dataset from an alternative “image-centric” point-of-view. Here, we are not as interested in the Raman spectrum itself but rather its use as a tool to enhance differences within the image or its image contrast.

In Figure 4, Raman images are presented in which the image contrast is generated by multivariate curve resolution (MCR) analysis. In this case, MCR finds the differences within each image and across the entire time sequence. A different color is assigned to each resolved component. This color use is analogous to using dyes in biological fluorescence imaging which tag different parts of a cell. Each image is from the same 30  $\mu\text{m}$  square portion of the anode. The blue MCR component is indicative of the 1580  $\text{cm}^{-1}$  band; green the 1590  $\text{cm}^{-1}$  band; yellow the 154  $\text{cm}^{-1}$  band; red represents carbon black, a conductivity enhancer.

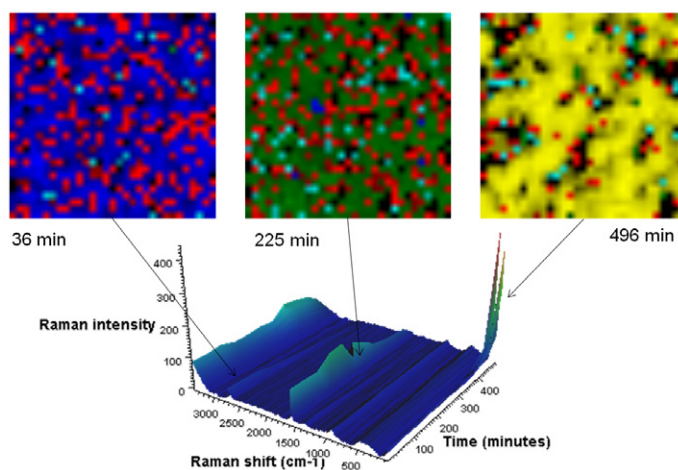


Figure 4. Raman images from different time slices in the graphite lithiation experiment.

It can be challenging to visualize the information content with such a massive wealth of data. Figure 4 shows just three frames to demonstrate this type of analysis. The changes are easy to grasp in the software. Please contact your local Thermo Fisher representative for a demonstration.

## Conclusion

The high sensitivity of Raman imaging is a benefit for Li-ion battery analysis. *In situ* Raman imaging techniques show the spatial distribution of phase changes in electrodes over time. This capability was not possible using single point measurements using traditional Raman microscopy.

The data were collected using an older model instrument, the DXRxi Raman Microscope. Currently, Thermo Fisher Scientific offers an improved model, the Thermo Scientific DXR3xi Raman Microscope, which offers superior speed and performance over its predecessor models.

## Authors

Dick Wieboldt, PhD, Thermo Fisher Scientific, Madison, WI, USA

Ines Ruff, PhD, Thermo Fisher Scientific, Dreieich, Germany

Matthias Hahn, PhD, El-Cell GmbH, Homburg, Germany

## Keywords

Electrodes, *In Situ* Analysis, Lithium Ion Battery, Raman Microscopy, Raman Imaging, DXR3xi Raman Imaging Microscope

## References

1. P. Tarte, *J. Inorg. Nucl. Chem.* 29(4) 915–923 (1967).
2. W.B. White, B.A. De Angelis, *Spectrochimica Acta Part A* 23(4) 985–995 (1967).
3. R. Baddour-Hadjean, J.P. Pereira-Ramos, *Chemical Reviews* 110(3) 1278–1319 (2010).
4. T. Gross, C. Hess, *J Power Sources* 256, 220–225 (2014).
5. P. Novák, D. Goers, L. Hardwick, M. Holzapfel, W. Scheifele, J. Ufheil, A. Wursig, *J Power Sources* 146, 15–20 (2005).
6. C.M. Burba, R. Frech, *Applied Spectroscopy* 60(5), 490–493 (2006).
7. E. Markevich, V. Baranchugov, G. Salitra, D. Aurbach, M. Schmidt, *J Electrochem Soc* 155(2), A132–A137 (2008).
8. Y. Luo, W.B. Cai, X.K. Xing, D.A. Scherson, *Electrochem. Solid-State Lett.* 7(1), E1–E5 (2004).
9. T. Gross, L. Giebeler, C. Hess, *Rev. Sci. Instrum.* 84(7), 073109-1–073109-6 (2013).
10. K. Hongyou, T. Hattori, Y. Nagai, T. Tanaka, H. Nii, K. Shoda, *Power Sources* 243, 72–77 (2013).
11. J. Lei, F. McLarnon, R. Kostecki, *J. Phys. Chem. B*, 109(2), 952–957 (2005).
12. <http://www.aimspress.com/article/10.3934/matersci.2018.4.650/Related.html>
13. <https://www.sciencedirect.com/science/article/abs/pii/S0378775317303531>

Learn more at [thermofisher.com/energy](https://thermofisher.com/energy)

thermo scientific

For research use only. Not for use in diagnostic procedures. For current certifications, visit [thermofisher.com/certifications](https://thermofisher.com/certifications)

© 2022 Thermo Fisher Scientific Inc. All rights reserved. All trademarks are the property of Thermo Fisher Scientific and its subsidiaries unless otherwise specified. AN52676-EN-03-2022